Electronic, Spectral, and Electrochemical Properties of ($TPPBr_x$)Zn Where $TPPBr_x$ Is the Dianion of β-Brominated-Pyrrole Tetraphenylporphyrin and *x* Varies from 0 to 8

Francis D'Souza,*,† Melvin E. Zandler,† Pietro Tagliatesta,*,‡ Zhongping Ou,§ Jianguo Shao,§ Eric Van Caemelbecke,§ and Karl M. Kadish*,§

Department of Chemistry, Wichita State University, Wichita, Kansas 67260-0051, Dipartimento di Scienze e Tecnologie Chimiche, II Università degli Studi di Roma, 00133 Roma, Italy, and Department of Chemistry, University of Houston, Houston, Texas 77024-5641

Received March 25, 1998

The electronic, spectral, and electrochemical characterization of (*meso*-tetraphenylporphyrinato)zinc(II) complexes bearing between 0 and 8 bromo substituents at the β-pyrrole positions is reported. The investigated compounds are represented as ($TPPBr_x$)Zn where $TPPBr_x$ is the dianion of brominated 5,10,15,20-tetraphenylporphyrin and *x* varies between 0 and 8. Each porphyrin undergoes four well-defined one-electron transfer reactions to yield porphyrin π-cation radicals and dications upon oxidation and porphyrin π-anion radicals and dianions upon reduction. Half-wave potentials for the first reduction of ($TPPBr_x$)Zn can be described by a single linear free energy relationship, and plots of $E_{1/2}$ versus the number of Br groups on the complex show a linear correlation with a positive slope of 63 mV per Br group. This is not the case for the other three electron transfer processes of the compounds where plots of $E_{1/2}$ versus the number of Br groups show distinctly different linear correlations for derivatives with 0−4 Br groups and those with 4−8 Br groups. The effect of increasing number of Br groups on the spectral and electrochemical properties of the neutral complexes was examined over the whole series of compounds, and these experimental results are compared to results of theoretical calculations by semiempirical molecular orbital AM1 methods using configurational interactions (CI) over the four Gouterman frontier π-orbitals. The dihedral angle containing the four porphyrin macrocycle ring nitrogens is proposed as a measure of porphyrin ring nonplanarity, and this value increases with increasing number of Br substituents on ($TPPBr_x$)Zn. Results of the AM1-CI = 4 calculations indicate that the spectrally determined HOMO−LUMO gap, i.e., the energy corresponding to the low-energy absorption band, varies in a nonlinear fashion with increasing number of Br substituents on the macrocycle and this is due to both the electronic effect of the substituents and the macrocycle nonplanarity. The HOMO−LUMO gaps theoretically calculated by AM1-CI = 4 methods thus parallel values which are experimentally obtained by electrochemistry or spectroscopy. The lack of well-defined linear free energy relationships for all processes except for the first reduction can be explained on the basis of electronic effects caused by the halogen substituents and nonplanar macrocyclic distortions induced by steric interactions among the peripheral substituents. In the case of porphyrin dication formation, the redox potentials are virtually independent of the bromo substituents.

Introduction

A number of papers have reported the properties of nonplanar porphyrins containing bulky or highly halogenated substituents at the β-pyrrole positions of the porphyrin macrocycle,[1−18] and several[19−23] have also modeled the effect of substituents by using semiempirical and ab initio calculations. Our own laboratories have examined the electrochemical and spectroscopic properties of ($TPPBr_x$)M where $TPPBr_x$ is the dianion of β-brominated 5,10,15,20-tetraphenylporphyrin, *x* = 0−8 and M = Fe or Co.[2,7,16,17] In accordance with theoretical predictions,[19−23] a

† Wichita State University.
‡ II Università degli Studi di Roma.
§ University of Houston.

(1) Ochsenbein, P.; Ayougou, K.; Mandon, D.; Fischer, J.; Weiss, R.; Austin, R. N.; Jayaraj, K.; Gold, A.; Terner, J.; Fajer, F. *Angew. Chem.* **1994**, *33*, 348.
(2) Kadish, K. M.; D'Souza, F.; Villard, A.; Autret, M.; Van Caemelbecke, E.; Bianco, P.; Antonini, A.; Tagliatesta, P. *Inorg. Chem.* **1994**, *33*, 5169.
(3) Ravikanth, M.; Chandrashekar, T. K. *Struct. Bonding (Berlin)* **1995**, *82*, 105.
(4) Traylor, T. G.; Tsuchiya, S. *Inorg. Chem.* **1987**, *26*, 1338.
(5) Bhyrappa, P.; Krishnan, V. *Inorg. Chem.* **1991**, *30*, 239.
(6) Mandon, D.; Ochsenbein, P.; Fischer, J.; Weiss, R.; Jayaraj, K.; Gold, A.; White, P. S.; Brigaud, O.; Battioni, P.; Mansuy, D. *Inorg. Chem.* **1992**, *31*, 2044.
(7) D'Souza, F.; Villard, A.; Van Caemelbecke, E.; Franzen, M. M.; Boschi, T.; Tagliatesta, P.; Kadish, K. M. *Inorg. Chem.* **1993**, *32*, 4142.
(8) Bhyrappa, P.; Nethaji, M.; Krishnan, V. *Chem. Lett.* **1993**, 869.
(9) Bhyrappa, P.; Krishnan, V.; Nethaji, M. *J. Chem. Soc., Dalton Trans.* **1993**, 1901.
(10) Watanabe, E.; Nishimura, S.; Ogoshi, H.; Yoshida, Z. *Tetrahedron* **1975**, *31*, 1385.
(11) Gong, L.-G.; Dolphin, D. *Can. J. Chem.* **1985**, *63*, 401.
(12) Gong, L.-G.; Dolphin, D. *Can. J. Chem.* **1985**, *63*, 406.
(13) Wu, G.-Z.; Gan, W.-X.; Leung, H.-K. *J. Chem. Soc., Faraday Trans.* **1991**, *87*, 2933.
(14) Callot, H. J. *Bull. Soc. Chim. Fr.* **1974**, *8*, 1492.
(15) Scheidt, W. R.; Lee, Y. J. *Struct. Bonding (Berlin)* **1987**, *64*, 1.
(16) Tagliatesta, P.; Li, J.; Autret, M.; Van Caemelbecke, E.; Villard, A.; D'Souza, F.; Kadish, K. M. *Inorg. Chem.* **1996**, *35*, 5570.
(17) Kadish, K. M.; Li, J.; Van Caemelbecke, E.; Ou, Z.; Guo, N.; Autret, M.; D'Souza, F.; Tagliatesta, P. *Inorg. Chem.* **1997**, *36*, 6292.
(18) For β-alkylated tetraarylporphyrins see: Shelnutt, J. A.; Song, X.-Z.; Ma J.-G.; Jia, S.-L.; Jentzen, W.; Medforth, C. J. *Chem. Soc. Rev.* **1998**, *27*, 31 and references therein.
(19) Takeuchi, T.; Gray, H. B.; Goddard, W. A., III. *J. Am. Chem. Soc.* **1994**, *116*, 9730.
(20) Brigaud, O.; Battioni, P.; Mansuy, D. *New. J. Chem.* **1992**, *16*, 1031.
(21) Hariprasad, G.; Dahal, S.; Maiya, B. G. *J. Chem. Soc., Dalton Trans.* **1996**, 3429.
(22) Ghosh, A. *J. Phys. Chem.* **1994**, *98*, 11004.
(23) Ghosh, A. *J. Am. Chem. Soc.* **1995**, *117*, 4691.

S0020-1669(98)00336-X CCC: $15.00
Published on Web 08/19/1998

nonlinear relationship is observed between potentials for the first ring- or metal-centered oxidation of each compound and the number of bromo substituents at the β-pyrrole position of the macrocycle. However, a linear relationship is obtained for potentials involving the first metal-centered reduction of the same series of compounds.

The occurrence or nonoccurrence of linear free energy relationships between $E_{1/2}$ and the number of Br groups on the porphyrin macrocycle can be explained on the basis of inductive effects caused by the electron-withdrawing halogen substituents as well as by nonplanar macrocyclic distortions induced by steric interactions among the peripheral substituents. However, only the first reduction and first oxidation have been examined in detail and little is known about how redox potentials for formation of porphyrin dications or dianions will be influenced by a systematic change in the total electronic effect of porphyrin ring substituents accompanied by simultaneous stepwise change from a planar to a slightly nonplanar to a very nonplanar porphyrin macrocycle. This is examined in the present study, which reports the spectral and electrochemical properties of zinc(II) tetraphenylporphyrins bearing between 0 and 8 bromo substituents at the β-pyrrole positions of the macrocycle.

The investigated compounds are represented as $(TPPBr_x)Zn$ where x varies between 0 and 8. Zinc(II) porphyrins were chosen because they are known to undergo only macrocycle-based oxidations and reductions, all of which are generally well-defined and all of which can be seen under the same solution conditions.[24] Thus, the data for these compounds can provide information on substituent effects involving highly charged nonplanar porphyrin macrocycles while, at the same time, being used to systematically probe the effects of increased β-bromination on the electrochemically and spectroscopically measured HOMO−LUMO energy gap. These data can also be compared to results of theoretical calculations on the same series of neutral compounds, which is another goal of the present study.

Experimental Section

Chemicals. Chloroform, used in the synthesis of the compounds, was distilled over P_2O_5 under nitrogen prior to use. *N*-Bromosuccinimide (NBS) was purified according to literature procedures.[25] Absolute dichloromethane (CH_2Cl_2), over molecular sieves, and tetra-*n*-butylammonium perchlorate (TBAP) were obtained from Fluka Chemical Co. Benzonitrile under sure seal bottles stored under argon were purchased from Aldrich Chemical Co. and used as such. TBAP was recrystallized from ethyl alcohol and dried under vacuum at 40 °C for at least 1 week prior to use. Ultrahigh-purity nitrogen gas, used to purge the solutions, was purchased from Trigas.

$(TPPBr_x)H_2$. Syntheses of the free-base β-brominated porphyrins with $x = 0-4$ and $6-8$ were performed according to literature procedures.[16]

$(TPPBr_5)H_2$. A 200 mg (0.2 mmol) sample of $(TPPBr_4)Zn$ (see below) was dissolved in dry chloroform to which 54 mg (0.3 mmol) of *N*-bromosuccinimide was added. The mixture was refluxed in air and protected by a $CaCl_2$ valve for 2 h, after which the solution was evaporated and the residue redissolved in 20 mL of chloroform. To this solution was added 10 mL of CF_3COOH under nitrogen, and the mixture was then stirred for 2 h. The reaction mixture was poured into ice−water, and the organic solution was separated from the mixture and washed with a saturated $NaHCO_3$ solution, after which it was dried over anhydrous Na_2SO_4 and evaporated to dryness. The residue was purified by column chromatography on silica gel, eluted with $CHCl_3$/*n*-hexane, 1:1. After recrystallization from $CHCl_3$/*n*-hexane, 1:3, 140 mg of pure $(TPPBr_5)H_2$ was obtained. Yield: 69.5%. ^{1}H NMR in $CDCl_3$, δ (ppm): 8.71 (1H, s, β-pyrrole), 8.62 (2H, s, β-pyrrole), 8.18−8.30 (8H, m, *o*-phenyl), 7.71−8.08 (12H, m, *m*- and *p*-phenyl). Mass (FAB/NBA): m/z 1008.5 $[M - H]^+$. Anal. Calcd for $C_{44}H_{25}N_4Br_5$: C, 52.47; H, 2.50; N, 5.55. Found: C, 52.60; H, 2.29; N, 5.70.

$(TPPBr_x)Zn$ ($x = 0-8$). About 100 mg of $(TPPBr_x)H_2$ was dissolved in pure chloroform, and 2 mL of saturated zinc acetate tetrahydrate in methanol was added under nitrogen. The solution was refluxed for 2 h, after which it was washed with water, dried over anhydrous Na_2SO_4, and evaporated to dryness. The residue was purified by column chromatography on silica gel and eluted with $CHCl_3$/*n*-hexane, 1:1. After recrystallization from $CHCl_3$/*n*-hexane, 1:3, pure products were obtained. Yields varied between 85 and 95%. ^{1}H NMR data, recorded in $CDCl_3$, δ (ppm), are as follows. $(TPPBr_1)Zn$: 9.16 (1H, s, β-pyrrole), 8.8−8.98 (6H, m, β-pyrrole), 8.12−8.38 (6H, m, *o*-phenyl), 7.98−8.10 (2H, d, *o*′-phenyl), 7.55−7.87 (12H, m, *m*- and *p*-phenyl). $(TPPBr_2)Zn$: 9.04 (2H, s, β-pyrrole), 8.82 (4H, s, β-pyrrole), 7.80−8.35 (8H, m, *o*-phenyl), 7.62−7.83 (12H, m, *m*- and *p*-phenyl). $(TPPBr_3)Zn$: 9.00 (1H, s, β-pyrrole), 8.85 (2H, s, β-pyrrole), 8.77 (2H, s, β-pyrrole), 7.80−8.13 (2H, m, *o*-phenyl), 7.78−810 (6H, m, *o*′-phenyl), 7.65−7.85 (12H, m, *m*- and *p*-phenyl). $(TPPBr_4)Zn$: 8.75 (4H, s, β-pyrrole), 8.01−8.15 (8H, m, *o*-phenyl), 7.68−7.82 (12H, m, *m*- and *p*-phenyl). $(TPPBr_5)Zn$: 8.65 (1H, s, β-pyrrole), 8.55 (2H, s, β-pyrrole), 8.02−8.23 (8H, m, *o*-phenyl), 7.68−7.78 (12H, m, *m*- and *p*-phenyl). $(TPPBr_6)Zn$: 8.78, 8.68, 8.55 (2H total (due to the presence of isomers), s, β-pyrrole), 8.02−8.22 (8H, m, *o*-phenyl), 7.70−7.95 (12H, m, *m*- and *p*-phenyl). $(TPPBr_7)Zn$: 8.51 (1H, s, β-pyrrole), 7.80−8.25 (8H, m, *o*-phenyl), 7.58−7.78 (12H, m, *m*- and *p*-phenyl). $(TPPBr_8)Zn$: 8.12 (8H, m, *o*-phenyl), 7.77 (12H, m, *m*- and *p*-phenyl). A summary of the elemental analyses and mass spectral data for the different $(TPPBr_x)Zn$ derivatives is given in Table 1 while the UV−visible spectral data are given in Table 2.

Table 1. Elemental Analyses and FAB Mass Spectral Data for $(TPPBr_x)Zn$ ($x = 1-8$)

	% C		% H		% N		*m/z*	
compd	calcd	found	calcd	found	calcd	found	calcd	found
$(TPPBr_1)Zn$	69.81	70.02	3.60	3.70	7.40	7.32	757	758.0
$(TPPBr_2)Zn$	63.22	63.15	3.14	3.32	6.70	6.82	835	835.0
$(TPPBr_3)Zn$	57.77	57.85	2.75	2.80	6.12	6.15	914	915.0
$(TPPBr_4)Zn$	53.18	53.20	2.43	2.54	5.64	5.70	994	995.0
$(TPPBr_5)Zn$	49.27	49.40	2.16	2.25	5.22	5.40	1073	1073.0
$(TPPBr_6)Zn$	45.90	45.95	1.93	2.10	4.87	4.97	1153	1153.0
$(TPPBr_7)Zn$	42.95	42.81	1.72	1.80	4.55	4.60	1230	1231.0
$(TPPBr_8)Zn$	40.36	40.44	1.54	1.60	4.28	4.20	1309	1310.0

Table 2. UV−Visible Spectral Data for $(TPPBr_x)Zn$ Complexes in PhCN

no. of Br	λ_{max} (nm) (molar absorptivity ($\epsilon \times 10^{-4}$))			
	Soret band	band I	band II	ϵ(I/II)[a]
0	427 (36.7)	556 (1.7)	597 (0.7)	2.4
1	430 (35.9)	560 (1.5)	601 (0.7)	2.1
2	434 (38.3)	564 (1.6)	603 (0.9)	1.8
3	438 (31.2)	571 (1.5)	611 (0.9)	1.7
4	439 (19.8)	569 (1.0)	613 (0.6)	1.7
5	446 (22.8)	579 (0.9)	626 (0.5)	1.8
6	461 (19.2)	601 (1.2)	653 (1.2)	1.0
7	471 (18.8)	609 (0.7)	671 (1.0)	0.7
8	477 (19.7)	622 (1.0)	685 (1.6)	0.6

[a] ϵ(I/II) is defined as the ratio of molar absorptivities for band I and band II.

Instrumentation. Mass spectra were obtained on a VG-4 mass spectrometer using *m*-nitrobenzyl alcohol (NBA) as the matrix. Elemental analyses were carried out at the Microanalysis Laboratory of the University of Padova, Italy. ^{1}H NMR spectra were recorded on an AM-400 Bruker instrument. UV−visible spectra were recorded with a Hewlett-Packard model 8453 diode array rapid scanning spectrophotometer.

Cyclic voltammograms were obtained with an EG&G model 173 potentiostat. Current−voltage curves were recorded on an EG&G Princeton Applied Research model RE-0151 X-Y recorder. A three-

(24) Kadish, K. M. *Prog. Inorg. Chem.* **1986**, *34*, 435.
(25) Perrin, D. D.; Armarego, W. L. F.; Perrin, D. R. *Purification of Laboratory Chemicals*, 2nd ed.; Pegamon Press: New York, 1980.

electrode system was used and consisted of a glassy carbon or platinum button working electrode, a platinum wire counter electrode, and a saturated calomel reference electrode (SCE). This reference electrode was separated from the bulk of the solution by a fritted-glass bridge filled with the solvent/supporting electrolyte mixture. All potentials are referenced to the SCE.

Computational Strategy. Semiempirical molecular calculations at the MNDO level were carried out with the MOPAC program[26] (versions 6.0 and 7.0) on a DEC ALPHA-station, DEC VAX-stations, and various PC's. The AM1 (Dewar) method[27] was employed. All isomeric structures were completely geometry optimized to a stationary point on the Born−Oppenheimer potential energy surface. At each stationary point, the following properties were automatically produced by the MOPAC program: the molecular wave function, orbital energies and Koopmans ionization potentials; the atomic charges, dipole moments, and bond orders; the bond distances and angles; and the heats of formation (relative energies).

At the geometry optimized structure (stationary point), a single point (1 SCF) configuration interaction was performed over the four frontier orbitals of Gouterman, which include two nearly degenerate HOMOs (b1 and b2 with a_{2u} and a_{1u} symmetries in D_{4h}) and two nearly degenerate LUMOs (c1 and c2 with e_g symmetry in D_{4h}).[28] This procedure yielded the energy, E_0, of the low-energy ground-state singlet, S_0, $(b1)^2(b2)^2$ and estimates of the energies for the next four lowest singlet states, E_1, E_2, E_3, and E_4. The transition energies associated with the visible bands, Q_1 and Q_2, and the Soret bands, B_1 and B_2, were obtained by difference, i.e., $Q_1 = E_1 - E_0$, $Q_2 = E_2 - E_0$, $B_1 = E_3 - E_0$, and $B_2 = E_4 - E_0$.

Semiempirical AM1 calculations were performed on the following isomers of each (TPPBr$_x$)Zn derivative: (TPP)Zn, one isomer; (TPPBr$_1$)Zn, one isomer (2-substituted); (TPPBr$_2$)Zn, three isomers (2,3-, 2,12-, and 2,13-substituted); (TPPBr$_3$)Zn, one isomer (2,3,12-substituted); (TPPBr$_4$)Zn, one isomer (2,3,12,13-substituted); (TPPBr$_5$)Zn, one isomer (2,3,7,12,13-substituted); (TPPBr$_6$)Zn, three isomers (2,3,7,8,12, 13-, 2,3,7,12,13,17-, and 2,3,7,12,13,18-substituted); (TPPBr$_7$)Zn, one isomer (2,3,7,8,12,13,17-substituted); (TPPBr$_8$)Zn, one isomer (2,3,7,8, 12,13,17,18-substituted).

Results and Discussion

Semiempirical Calculations. Semiempirical methods form an important middle ground between molecular mechanics and the elaborate ab initio MO calculations[29] and have been used extensively in recent years for studying the structures, properties, and reactions of porphyrin molecular systems.[19−21] It is known that AM1 methods will predict molecular geometry, orbital energies, and charge distribution of large organic systems as accurately as medium-level ab initio methods[29−31] (HF/321G* or higher) and better than low-level ab initio procedures (STO-3G). Since first ionization potentials were used in the parametrization of AM1, the orbital energies agree well with photoelectron spectroscopy experiments. Charge distributions are realistic due to the use of experimental dipole moment information. Relative energies, especially for isomeric species, are quite well predicted, whereas absolute energies, as represented by heats of formation, vary in accuracy between procedures. Lower level ab initio SCF procedures, e.g. STO-3G, are expected to be inapplicable or inspire little confidence for delocalized systems of the size treated here. Higher level ab initio calculations beginning with HF/6-31G* would be expected to be reliable but would overestimate bond alternation as does AM1. Post-SCF and/or DFT methods may be necessary to fully represent the delocalized tetrapyrrole and especially the electronic environment of the cavity, but they are not practical tools for molecules of this size with no symmetry.

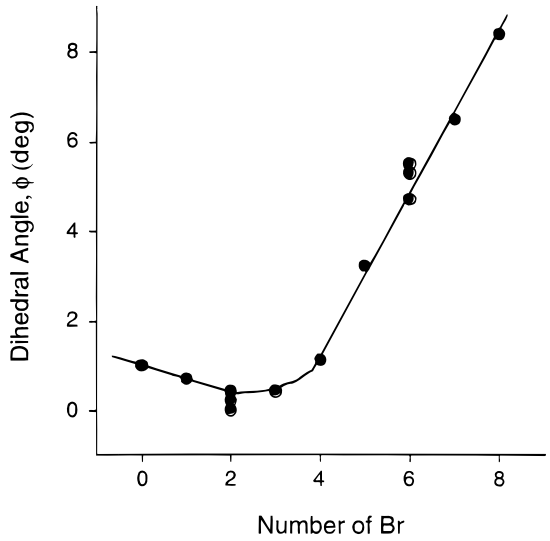

Figure 1. Plot of the dihedral angle, ϕ, of the four ring nitrogens versus the number of Br substituents on the macrocycle.

For AM1 optimized structures of the partially brominated porphyrins, it was observed that the ring nonplanarity is nonuniform with respect to the four pyrrole rings (C_1 point group); i.e., the pyrrole rings bearing two Br substituents deviated more from the plane of the porphyrin than the pyrrole rings having either one or no Br substituents. An attempt was made to estimate the degree of ruffling with respect to different brominated porphyrin derivatives on the AM1 optimized structures. To accomplish this, we have evaluated the dihedral angle, ϕ, containing the four ring nitrogens of the fully optimized structures by AM1 methods. It was assumed that the pyrrole ring bearing two bromo substituents rotates along the C_{meso} axis to cause the nonplanarity. Such a rotation along the C_{meso} axis would result in a displacement of the C_β carbons (and the attached Br groups) out of the mean porphyrin plane while the ring nitrogens would move in the same direction but to a smaller degree than that of the C_α carbons in the porphyrin plane. A measurement of the dihedral angle containing the four ring nitrogens should then give an estimate of the overall nonplanarity.

Figure 1 shows how the dihedral angle of (TPPBr$_x$)Zn varies with the number of Br groups and suggests that the effect of macrocycle nonplanarity begins to occur with the tetrabrominated derivatives, after which the dihedral angle (and nonplanarity of the macrocycle) increases in a linear fashion with increasing number of Br substituents on the porphyrin. The increase of nonplanarity with the number of Br substituents on the porphyrin macrocycle has been demonstrated by crystal structures for related tetra- and octabrominated *meso*-tetramesitylporphyrin derivatives.[1]

Table 3 lists the energy of the first four singlet−singlet transitions (Q_1, Q_2, B_1, and B_2), the calculated heats of formation, ΔH_f, and the values of the dipole moment for different isomers of (TPPBr$_x$)Zn while Figure 2 shows AM1 calculated spectral trends for the Q_1 (visible) band as a function of the number of Br groups. The Q_1 band represents an electronic transition between the low-energy ground state and the first excited singlet state of (TPPBr$_x$)Zn. To differentiate spectral perturbations caused by a nonplanarity of the macrocycle from those due to

(26) *MOPAC. A General Molecular Orbital Package (QCPE Program No. 455)*; The Quantum Chemistry Program Exchange, Department of Chemistry, Indiana University: Bloomington, IN, 1990.
(27) Dewar, M. J. S.; Zoebisch, E. G.; Healy, E. F.; Stewart, J. J. P. *J. Am. Chem. Soc.* **1985**, *107*, 3902.
(28) Gouterman, M. *J. Mol. Spectrosc.* **1961**, *6*, 138.
(29) Hehre, W. J. *Practical Strategies for Electronic Structure Calculations*; Wavefunction Inc.: Irvine, CA, 1995.
(30) Dewar, M. J. S.; Storch, D. M. *J. Am. Chem. Soc.* **1985**, *107*, 3898.
(31) Dewar, M. J. S. *J. Phys. Chem.* **1985**, *89*, 2145.

Table 3. Results Obtained from AM1-CI = 4//AM1[a] Calculations for $(TPPBr_x)Zn$ Compounds

compd	isomer	ΔH_f[b] (kcal mol^{-1}) optimized	ΔH_f[b] (kcal mol^{-1}) planar[d]	ϕ[c] (deg)	dipole moment (D)	Q_1 (eV) optimized	Q_1 (eV) planar[d]	Q_2 (eV)	B_1 (eV)	B_2 (eV)
(TPP)Zn		390.85	390.91	1.0	0.05	2.297	2.299	2.303	3.667	3.692
$(TPPBr_1)Zn$	2-	397.97	397.99	0.7	1.82	2.306	2.308	2.313	3.660	3.693
$(TPPBr_2)Zn$	2,3-	405.71	405.93	0.2	3.23	2.303	2.313	2.311	3.617	3.648
	2,12-	406.37	406.40	0.4	0.40	2.293	2.293	2.315	3.666	3.709
	2,13-	406.41	406.45	0.0	1.18	2.299	2.300	2.309	3.666	3.710
$(TPPBr_3)Zn$	2,3,12-	414.19	414.38	0.4	2.06	2.294	2.300	2.308	3.627	3.670
$(TPPBr_4)Zn$	2,3,12,13-	423.24	423.41	1.1	1.17	2.280	2.285	2.307	3.629	3.689
$(TPPBr_5)Zn$	2,3,7,12,13-	433.16	433.65	3.2	1.81	2.274	2.280	2.286	3.585	3.654
$(TPPBr_6)Zn$	2,3,7,8,12,13-	442.43	444.77	4.7	2.24	2.219	2.260	2.263	3.486	3.506
	2,3,7,12,13,17-	443.35	443.35	5.3	0.96	2.266	2.281	2.271	3.564	3.599
	2,3,7,12,13,18-	443.12	444.10	5.5	1.63	2.269	2.280	2.269	3.564	3.610
$(TPPBr_7)Zn$	2,3,7,8,12,13,17-	452.74	455.80	6.5	1.16	2.221	2.262	2.256	3.483	3.512
$(TPPBr_8)Zn$	2,3,7,8,12,13,17,18-	463.22	468.14	8.4	0.31	2.217	2.258	2.239	3.483	3.498

[a] 1 SCF AM1-CI = 4 calculation for the fully optimized AM1 structure. [b] Heats of formation from the AM1 method. [c] Dihedral angle between the four nitrogen atoms. [d] The central zinc, the four porphyrin ring nitrogens, and the 20 porphyrin ring carbons are all held in one plane.

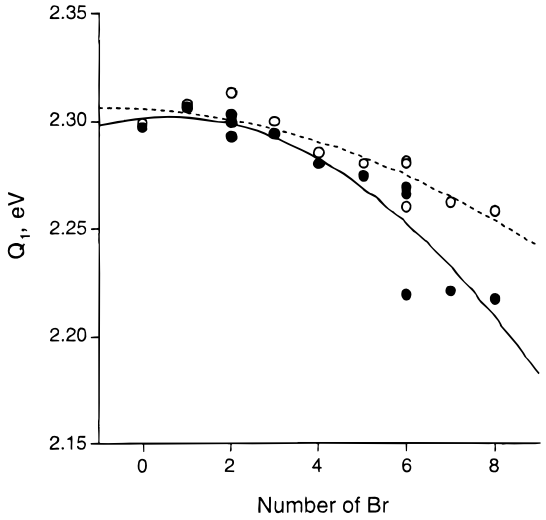

Figure 2. Plot of AM1 excitation energy corresponding to the Q_1 transition versus the number of Br groups on the porphyrin. The dashed line represents the trend for porphyrin derivatives with a planar configuration (○), while the solid line represents the trend for the fully AM1 optimized porphyrin derivatives (●).

electronic effects of the Br substituents, the transition energies were estimated by forcing the geometry of $(TPPBr_x)Zn$ into a planar configuration. To do this, the central zinc ion, the four porphyrin ring nitrogens, and the 20 porphyrin ring carbons were all held in one plane. The resulting spectral data for the Q_1 band would then be associated only with electronic effects caused by the Br substituents and not by a nonplanarity of the macrocycle. This plot is also included in Figure 2 and represented by open circles.

A comparison between data for porphyrins with a planar configuration (open circles in Figure 2) and those for fully AM1 optimized derivatives (solid circles in Figure 2) suggests that there is a substantial decrease in transition energy due to nonplanarity of the macrocycle. This effect is clearly seen for the $x = 7$ and 8 derivatives, while for the $x = 6$ derivative, the 2,3,7,8,12,13-isomer shows the highest decrease in energy. For brominated porphyrin derivatives with x ranging between 2 and 5, the lowering of the transition energy due to nonplanarity is also seen but this effect is much smaller. The large Q_1 transition energy for compounds forced to be in a planar configuration is due primarily to the more extensive lowering of the ground-state energy by CI of the planar systems, while small CI effects are seen on the upper states.

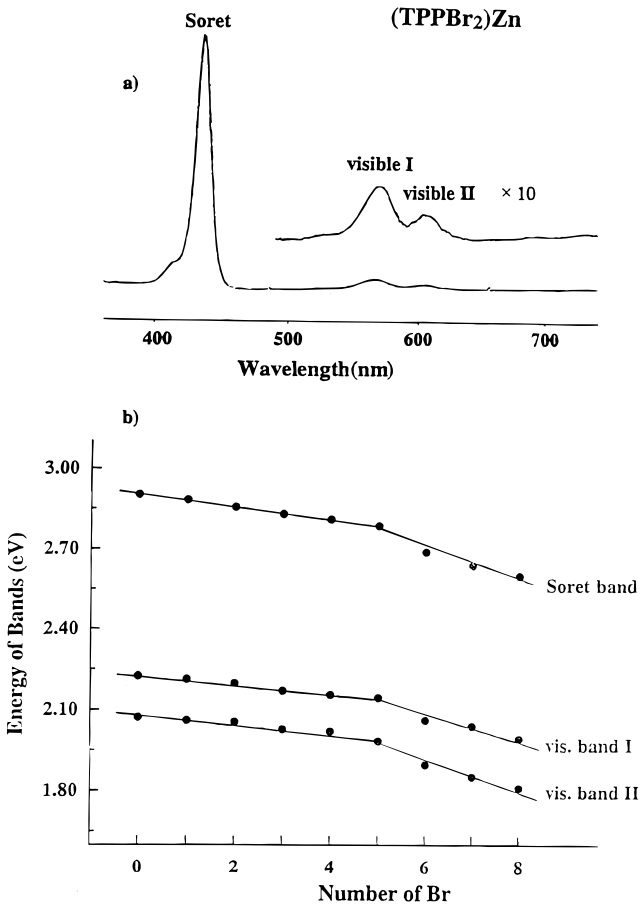

Figure 3. (a) UV−visible spectrum of $(TPPBr_2)Zn$ in benzonitrile, 0.1 M TBAP, and (b) plots of the absorption band energy versus the number of Br groups on the macrocycle of $(TPPBr_x)Zn$.

Similar spectral trends are observed for transitions involving higher excited states (see Table 3), and semiempirical calculations performed on the different isomers of $(TPPBr_x)Zn$ thus suggest that the red shift in absorption bands of the higher brominated porphyrins can be attributed to both an electronic effect of the Br groups and a nonplanarity of the macrocycle caused by steric factors. Results obtained by electrochemical and spectral studies, discussed below, agree well with these predictions.

Optical Spectroscopy. The semiempirical AM1-CI results suggest that the Soret and visible absorption bands of the porphyrins are highly sensitive to distortion of the porphyrin

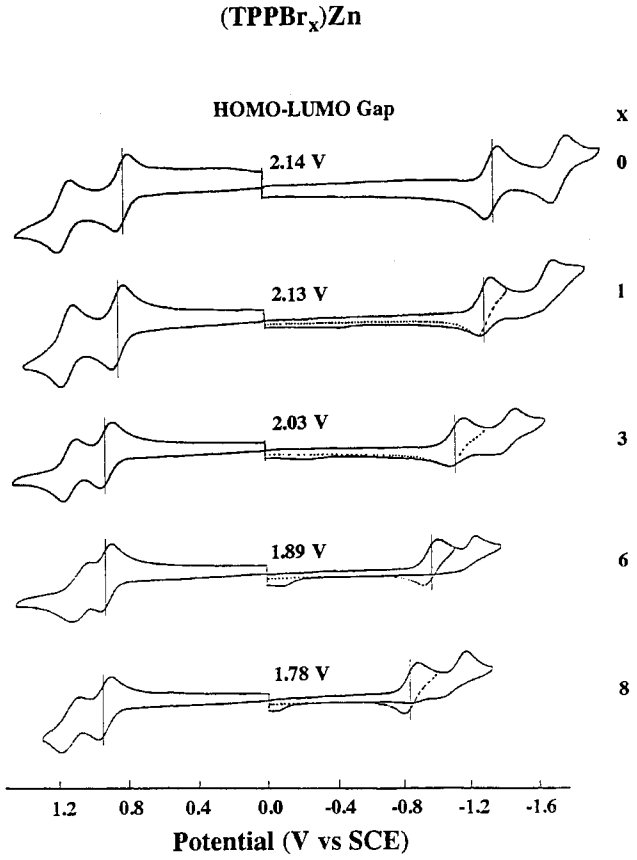

Figure 4. Cyclic voltammograms of representative (TPPBr$_x$)Zn complexes in PhCN, 0.1 M TBAP.

ring caused by peripheral substitution. Hence, one can quantitatively probe the porphyrin geometry by measuring wavelengths and molar absorptivities of each (TPPBr$_x$)Zn derivative as a function of the number of Br groups on the macrocycle. The electronic absorption spectrum of (TPPBr$_2$)Zn is shown in Figure 3a, while UV−visible data for each compound in benzonitrile are summarized in Table 2. As seen in this table, there is a systematic red shift in λ_{max} of each band upon increasing the number of Br groups in the complex. As the number of Br groups in (TPPBr$_x$)Zn is increased from 0 to 8, the molar absorptivities of both the Soret and visible band I decrease in magnitude, whereas the molar absorptivity of the visible band II increases.

Figure 3b illustrates how the energy of each absorption band shifts as a function of the number of Br groups in (TPPBr$_x$)Zn. Each band shows two linear segments with different slopes. The energy change per added bromo substituent, i.e., the slope of the plot, is larger for the x = 4−8 segment than for the x = 0−4 segment, and this result agrees with the predictions of AM1-CI = 4 calculations.

Electrochemistry. Cyclic voltammograms for representative (TPPBr$_x$)Zn complexes in benzonitrile containing 0.1 M TBAP are illustrated in Figure 4, and a summary of half-wave potentials in PhCN or CH_2Cl_2 is given in Table 4. Each porphyrin undergoes two well-defined one-electron oxidations and two well-defined one-electron reductions in both utilized solvents. The voltammograms of the brominated porphyrins have shapes similar to those of the unbrominated (TPP)Zn, and the four electrode reactions of each compound can be unambiguously assigned to formation of porphyrin π-cation radicals and dications upon oxidation and π-anion radicals and dianions upon reduction.[24]

Table 4. Half-Wave Potentials (V vs SCE) for Reduction and Oxidation of (TPPBr$_x$)Zn in Nonaqueous Solvents Containing 0.1 M TBAP

no. of Br atoms	oxidation 2nd	oxidation 1st	ΔE_{ox}	reduction 1st	reduction 2nd	ΔE_{red}	HOMO−LUMO gap $\Delta E_{1/2}$(1st ox−1st red)
PhCN Solvent							
0	1.14	0.82	0.32	−1.32	−1.74	0.42	2.14
1	1.18	0.88	0.30	−1.25	−1.68	0.43	2.13
2	1.17	0.91	0.26	−1.19	−1.58	0.39	2.10
3	1.16	0.93	0.23	−1.10	−1.42	0.32	2.03
4	1.19	0.95	0.24	−1.03	−1.32	0.29	1.98
5	1.15	0.96	0.19	−0.97	−1.28	0.31	1.93
6	1.11	0.96	0.15	−0.93	−1.20	0.27	1.89
7	1.14	0.97	0.17	−0.92	−1.15	0.23	1.89
8	1.15	0.96	0.19	−0.82	−1.15	0.32	1.78
CH_2Cl_2 Solvent							
0	1.11	0.78	0.33	−1.39	−1.84[a]	0.45	2.17
1	1.10	0.82	0.28	−1.26	−1.68[a]	0.42	2.08
2	1.09	0.84	0.25	−1.18	−1.56[a]	0.38	2.02
3	1.09	0.86	0.23	−1.11	−1.47[a]	0.36	1.97
4	1.14	0.90	0.24	−1.09	−1.36[a]	0.27	1.99
5	1.08	0.87	0.21	−1.04	−1.28[a]	0.24	1.91
6	1.08	0.85	0.23	−0.95	−1.24[a]	0.29	1.80
7	1.07	0.86	0.21	−0.90	−1.13[a]	0.23	1.76
8	1.11	0.85	0.26	−0.85	−1.10[a]	0.24	1.70

[a] E_{pc} at a scan rate of 100 mV/s.

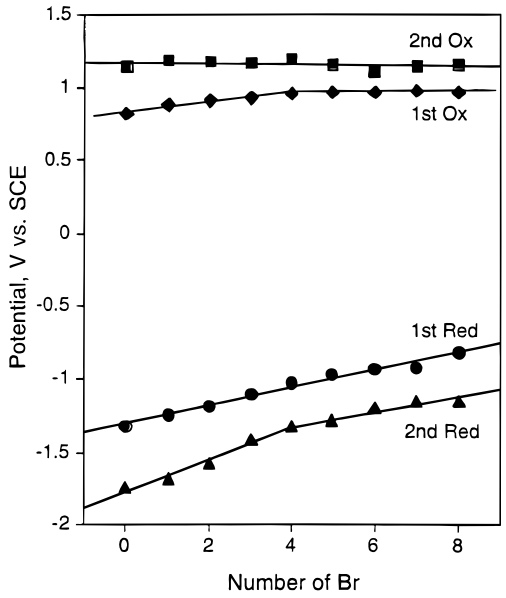

Figure 5. Dependence of the redox potentials on the number of bromo substituents for the four electrode reactions of (TPPBr$_x$)Zn.

Plots of $E_{1/2}$ versus the number of Br substituents on (TPPBr$_x$)Zn are illustrated in Figure 5 for the four electrode reactions in benzonitrile. The first oxidation consists of two linear segments, the first of which involves compounds with 0−4 Br groups and the second of which those with 4−8 groups. This parallels the spectroscopic data in Figure 3b as well as results earlier reported for (TPPBr$_x$)Co and (TPPBr$_x$)FeCl,[2,7,16,17] two series of compounds which have the same set of Br-substituted macrocycles. The second oxidation of (TPPBr$_x$)Zn shifts in a negative direction with increase in the number of Br substituents, but this reaction exhibits a quite small substituent effect of the Br groups.

The absolute potential difference between the two oxidations of (TPPBr$_x$)Zn is given by $\Delta E_{1/2}$(2−1) and decreases from 0.32 V for x = 0 in PhCN to 0.15 V for x = 6 under the same solution conditions. A similar result has been reported for (TPPBr$_x$)Co in PhCN, 0.1 M TBAP, where the potential separation between the second and third oxidations was shown to decrease with increase in the number of Br groups.[17]

A single linear free-energy relationship is seen between $E_{1/2}$ and the number of Br substituents for the first electroreduction, independent of the number of Br groups on (TPPBr$_x$)Zn. The slope of the plot is 63 mV/Br group (see Figure 5), and this value compares with a slope of 64 mV/Br for the first reduction of (TPPBr$_x$)Co[7,17] and 51 mV/Br for the first reduction of (TPPBr$_x$)Fe.[2,16] The second reduction of (TPPBr$_x$)Zn shifts in a positive direction with increase in the number of Br substituents, but two linear segments are seen in this case and the effect of substituents is decreased for compounds having more than 4 Br groups on the macrocycle. The absolute potential difference between the two reductions of (TPPBr$_x$)Zn in benzonitrile is given by $\Delta E_{1/2}(2-1)$ and decreases from 0.42 V in the case of $x = 0$ to 0.27 V in the case of $x = 6$.

The electrochemically measured HOMO−LUMO gap of (TPPBr$_x$)Zn in PhCN is given by $\Delta E_{1/2}$(1st ox−1st red) in Table 4. This value ranges from 2.14 V in the case of $x = 0$ to 1.78 V in the case of $x = 8$. A similar range of values is seen for the same series of compounds in CH_2Cl_2. The electrochemical results parallel data from theoretical calculations using the AM1-CI method and are also consistent with earlier calculations performed by other groups on nonplanar porphyrins.[19−21] The experimental and theoretical results are thus self-consistent and indicate that the electronic effect of the Br substituents decreases the energies of both the HOMO and LUMO orbitals but that the stabilization of the orbital energies is counterbalanced by a distortion of the macrocycle, which leads to a destabilization of the porphyrin HOMO orbitals without significantly affecting the energy of the LUMO orbitals.

A comparison between the HOMO−LUMO energy gaps obtained in the present study using different methods is shown in Figure 6. All three analyses lead to plots with two linear segments and a break for compounds with 2, 3, or 4 Br groups. The slope of the linear segment in the plot of calculated HOMO−LUMO gap versus the number of Br groups on the macrocycle is larger for compounds with $x > 4$ than for compounds with $x < 4$. Figure 6 also indicates that the AM1-CI method leads to a calculated decrease in the HOMO−LUMO gaps upon going from compounds with $x = 0$ to $x = 8$, but the decrease is smaller than the decrease determined experimentally for the same series of compounds by either spectroscopy or electrochemistry. This suggests that solvation might play a role in stabilizing the HOMO and/or LUMO orbitals of the nonplanar porphyrins since data calculated by the AM1-CI method involve reactions of the compounds in the gas phase. Higher level ab initio calculations which include solvation parameters might overcome this discrepancy.

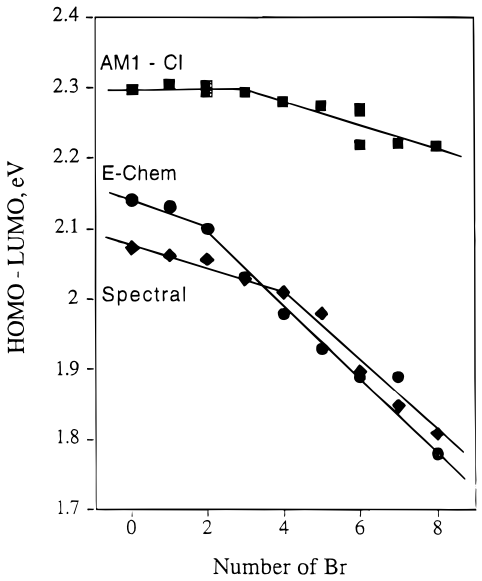

Figure 6. Correlations between the calculated or experimental HOMO−LUMO gap of each compound and the number of Br substituents on the macrocycle.

Acknowledgment. The support of the Robert A. Welch Foundation (Grant E-680, K.M.K.) as well as the donors of the Petroleum Research Fund, administered by the American Chemical Society (F.D.), is gratefully acknowledged. The Italian CNR is also acknowledged (P.T.) for a travel grant.

IC980336Y